Leaf Vein Structure in Additively Manufactured Aluminium Components for Stiffness

Jyothirmay Bhattacharjya ⓘ**, Meenakshi Devi Parre** ⓘ**, and Vamsi Krishna Pasam** ⓘ

1   Introduction

Additive manufacturing (AM) is one of the emerging trends in the manufacturing sector. The complex part manufacturing capabilities as well as its ability to produce high-quality products with minimum loss of material makes it a versatile technique. A number of additive manufacturing techniques are commercially available nowadays for both polymer and metal 3D printing. Some of them are selective laser melting (SLM), fused deposition modelling (FDM) and electron beam melting (EBM). However, process parameters selection is a tedious task to obtain the products with desired quality. A good set of process parameters can reduce the errors of the production process to a great extent. A lot of process parameters were observed from the literature of AM technology, among which some are interdependent also. Fused deposition modelling (FDM) is a widely adopted process that works on this technology [1]. In this technology generally, the material is used in the form of solid and with the help of some heating source it is melted and then extruded through a nozzle, like in the case of icing. The popular heat source used is induction heating. This technology is more popular for polymers like thermoplastics. The raw material can be used in the form of a spool of wire or small pieces of wire. For continuous feeding of the material, spool of wire is preferable. With the help of some roller mechanism, the wire is pulled inside the heating chamber. If the material is used in

J. Bhattacharjya
Department of Mechanical Engineering, National Institute of Technology, Warangal, Telangana 506004, India

M. D. Parre (✉) · V. Krishna Pasam
Department of Mechanical Engineering, RGUKT, RK Valley, YSR Kadapa(Dt), Andhra Pradesh, Idupulapaya 516330, India
e-mail: pmeenakshidevi@gmail.com

V. Krishna Pasam
e-mail: vamsikrishna@nitw.ac.in

any form other than a spool of wire, then it has to feed inside the heating chamber manually. Within the heating chamber, the material will be melted and it will be extruded through the nozzle. The nozzle is allowed to move in XY axis, while the building platform is allowed to move in Z-axis. Each layer will be fabricated by the XY direction movement of the nozzle. After printing one layer, the platform lowers down by the thickness of one layer and then again extrusion started. The speed at which material is extruded is a very important parameter for obtaining a good quality product.

The influence of nozzle temperature and infill line orientations for parts made with short carbon fibre (CF)-reinforced polylactic acid (PLA) is studied [2]. They proved the influence of nozzle temperature on the mechanical properties, with an optimum temperature maximizing the tensile properties. The addition of a reinforcing agent such as CF in the polymer matrix also improves the tensile properties if the process parameters are well chosen. The influence of the raster angle and the moisture content percentages on the mechanical properties of 3D-printed polylactic acid (PLA) material is studied [3]. This research specifies that specimens with a 90° raster angle and 10% moisture content have the optimum strength and strain mechanical properties. Three different types of polymers, including polylactic acid (PLA), polyethylene terephthalate glycol (PETG) and acrylonitrile butadiene styrene (ABS), were used in fused deposition modelling (FDM) process to fabricate several parts results of statistical analysis indicated the temperature as the significant factor on tensile strength while the material change did not show a significant effect [4]. A methodology for optimizing both process efficiency, i.e. time and energy consumption, and part quality, i.e. surface roughness and dimensional accuracy, of polylactic acid (PLA) components produced by FDM and it is shown that, according to the context, different parameter settings pursue different goals in terms of part quality and process efficiency[5]. The proposed approach may effectively help designers determine process parameters' settings to optimize both part quality and process efficiency and can be applied to either prototype or part production. The impact of FDM fabricated parts made up of ABS and the influence of build direction on mechanical properties is studied [6]. The parts are made with and without a hole in the centre. The parts were built in C + 45 orientation, XY and XZ directions. It was concluded from the study that parts fabricated in XZ direction have higher fracture strength and C + 45 has a lower strength. Parts without a hole are significantly affected by build direction. The change in dimension of the hole both in diameter and in-depth affects the fracture strength of the parts. The effect of process parameters on mechanical properties on 3D-printed PLA parts is studied [7]. Layer thickness of 0.1, 0.12, 0.15, 0.18 and 0.2 mm and orientation of 00, 180, 450, 720 and 900 are considered. The study identified that the ultimate tensile strength of the part decreased as the infill orientation reaches 900. The strength of the parts increased with an in-layer thickness to the value of 0.18 mm.

The effect of the external perimeter on FDM fabricated parts is studied [8]. Contour number, layer thickness, raster width, part orientation, raster angle and air gape were the factors considered in the study. It was observed that as the external perimeter is increased, the strength of the parts also increased. This is attributed to the shift in stress

concentration towards the centre due to the addition of contours. The combination of contour number = 5, layer thickness = 0.330 mm, raster width = 0.4064 mm, part orientation = 00, raster angle = 00 and air gape = 0 mm is found to give best results.

The mechanical properties are studied and compared the same among the alloy manufactured by selective laser melting (SLM), laser direct deposition (LDD) and electron beam melting (EBM) [9]. The mechanical properties of AM Ti alloys manufactured by different techniques are identified [10]. The author also studied the surface roughness, wear properties of AM alloys in comparison with wrought alloys. The complex relationship between AM processes, microstructure and resulting properties for metals is described [11]. Special attention is paid to AM specific grain structures. Micromilling of Ti alloys manufactured by conventional as well as AM techniques is focussed [12]. The surface finish, cutting forces and burr formation were studied. The microstructural and mechanical properties variation among different AM techniques were highlighted [13]. It also highlights the manufacturers of AM equipment.

In this work to improve the mechanical properties, bionically inspired structures are introduced into the samples. The stiffness of different thermoplastics is relatively low and it can be improved by the introduction of carbon fibres into it [14]. Two thermoplastics polylactic acid (PLA) and acrylonitrile butadiene styrene (ABS) were studied. Parts were fabricated using 3D printing technology and subjected to three-point bending test. The sample was made up of PLA, ABS, PLA reinforced with carbon fibres and ABS reinforced with carbon fibres. PLA reinforced with carbon fibres had the highest stiffness value followed by the unreinforced PLA and unreinforced ABS had the least value of stiffness. PLA material has a higher value of stiffness than ABS. A bionically inspired topological optimization to improve the stiffness for the column of a grinding machine is used [15]. Earlier due to the manufacturing constraints generally '#' and 'x' shaped stiffener layouts are used to improve the stiffness. There are three levels in which analogical analysis should be considered, those are structure, i.e. topology or shape, loading and functional similarity. These bionic structures can be used to solve engineering problems only if it satisfies the analogy. A leaf can be assumed as a cantilever subjected to the loadings due to the environmental impact and dead weight. The leaf vein structures are generally classified into two categories depending upon the number of principal veins, which are pinnate venation and palmate venation. The pinnate venation system used to have only one principal vein, while the palmate venation system used to have two principal vein structures. Improvisation of the stiffness with the help of a sandwich structure containing two thin, stiff face sheets of carbon fibre reinforced polymer and a thick low density porous structure is done [16]. The stiffness was improved remarkably with this model. This model was inspired by biological tissue structures. One problem with this type of sandwich structure is it is subjected to local failure, which limited its mechanical properties. The local failure includes debonding between the face and the core, and the core may collapse sometime. But this type of limitation in mechanical properties can be avoided by the use of structures like veins inside the sandwich structure. In nature, both grass leaves and tree leaves have the sandwich kind of tissue structure but the tree leaves are stronger than the grass leaves due

to the presence of vein structures in them. An approach to improve the mechanical properties of the parts fabricated by fused deposition modelling is proposed [17]. Thermally expandable microspheres were used in the matrix during fabrication and later on exposed to temperature increase due to which the microsphere expanded and occupied the voids in the parts. Positive results were observed for tensile strength. The addition of 2 weight% microspheres and heating at a temperature of 1400 C for 120 s improves the tensile strength of the parts by 25.4% than the untreated samples. The prime material used for FDM machines is ABS and PLA which are having melting temperatures in the range of 1800 C to 2200 C and the microspheres need heating at a temperature of 1400 C; hence, these microspheres effectively can be used without distortion of the main part during heat treatment.

In this work, simulation of the sample made up of PLA is done in ANSYS Workbench and the simulation results are obtained. Then, sample with the same dimensions as per ASTM D790 and made of PLA is fabricated in FDM and simulation and experimental details are validated. After the validation of results to check material dependency of leaf vein structures, an attempt is made to simulate the effect of different leaf vein structures on the strength of aluminium 6061-T6 alloy. Three-point bending test is used in this work to determine the strength of the sample. This work also emphasizes the role of bionically inspired structures in improving the design and strengthening the existing components by reducing stress and deformation. In addition, the design and fabrication of bionic structure reinforced additive manufactured components provides a new method of improving the mechanical properties of components produced by the aforementioned technique.

2   Design and Simulation

2.1   Fabrication of Standard Sample

After slicing and generating the G-code in the Flash Print, parts were fed to a Flash Forge printer. The standard specimen was fabricated, i.e. the rectangular bar without any vein structure. The specimen is fabricated according to ASTM D790 standard [18] with 127 mm long, 12.7 mm wide and 3.2 mm thick as in Fig. 1. The material used during fabrication is white polylactic acid (PLA), which is a widely used thermoplastic material for 3D printing machines. Some of the important specifications of the Flash Forge printer used for fabrication are listed in Table 1 and is shown in Fig. 2.

2.1.1   Steps in the Design of Vein Structures

The step-by-step process of how the veins are designed is described for arcuate vein structure. The same process is used for designing the other vein structures.
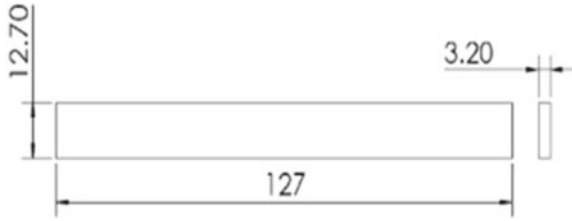
Fig. 1 Test specimen

Table 1 Specification of the Flash Forge printer used

S. No	Specification	Details
1	Print speed	40–60 mm/s
2	Layer resolution	100–300 microns
3	Nozzle temperature	220 °C
4	Build volume	$140 \times 140 \times 140$ mm^3
5	Nozzle diameter	0.4 mm
6	Product dimension	$420 \times 420 \times 420$ mm^3
7	Extruder	Single
8	Filament diameter	1.75 mm
9	Supported filament	PLA
10	File type	.stl,.obj
11	Software	Flash print

Fig. 2 Line diagram of FDM
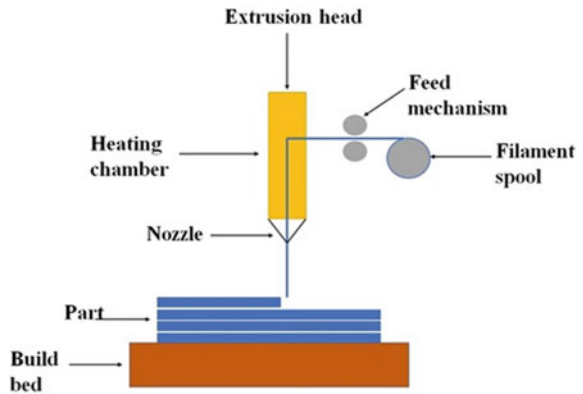
- At the start of the design, the type of modelling and unit for the dimensions has to select. The type of modelling selected was solid part and the unit selected was mmks.
- After setting the unit, the plane for drawing has to select. The front view was selected to draw the cross section of the rectangular bar.

- After selecting the plane, the sketch mode has to be selected where the primitive structures are present to draw the 2D profiles.
- For this model, the rectangular primitive was selected and the cross section was drawn in the front view. The dimension of the rectangle is 127 mm long and 12.7 mm wide.
- After obtaining the 2D cross section of the rectangular bar, it has to be extruded to get the 3D model. For this, the extrude command should be used. The cross section was extruded by 3.2 mm to get the rectangular bar of dimension 127 × 12.7 × 3.2 mm.
- After getting the rectangular bar, one of its faces has to be selected to draw the leaf veins on it using the spline command. Using spline command if veins are drawn, the advantage is that more control points are obtained on the vein to give it desired shape.
- After drawing all the primary, secondary and tertiary veins on the selected plane, the 3D shape was given to the drawn veins using swept blend command. This command helps in sweeping a cross section over an axis ununiformly.
- The cross section selected for the veins was circular with an initial diameter of 1.5 mm that converges to 1.2 mm for primary veins using the swept blend command. Similarly, for secondary veins, 0.8 mm converges to 0.6 mm and for tertiary veins; 0.6 mm converges to 0.4 mm.
- After sweeping the cross section of all the veins, the 3D model was ready for further use.

2.2 Three-Point Bending Test

In this work, three-point bending test was carried out to study the load vs. deformation behaviour of the standard sample, i.e. the one without any vein structure and with different vein structures. The schematic representation of three-point bending is shown in Fig. 3. Moreover, the data obtained from the experiment were used to find the flexural strength of the parts. The deflection of the sample was allowed until the rupture. It is used to get the modulus of elasticity in bending, flexural stress, flexural strain and flexural stress–strain response of the fabricated PLA sample. The elastic modulus in bending (E) can be extracted from a flexural test. The advantage of the flexural test comes from the ease of sample preparation and testing. However, the disadvantage comes from the fact that the results of the testing method are sensitive to specimen and loading geometry and strain rate. In the experiment, the sample was kept in the flat position on adjustable support. Then, the sample was loaded with the help of a moving crosshead located in between the support. The dimension of the test specimen is 127 mm long, 12.7 mm width and 3.2 mm thick and the support span length used here is 102 mm, according to ASTM D790. Total three samples were tested. The mechanical properties of the samples are given in Table 2.
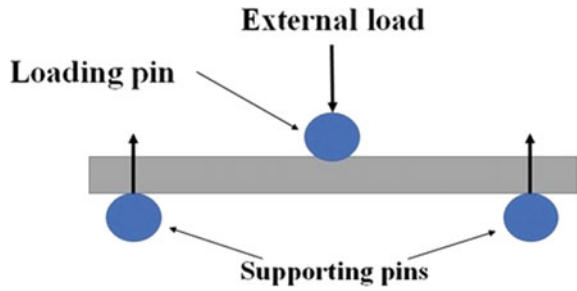
Fig. 3 Three-point bending test

Table 2 Average mechanical properties of all the samples

S.No	Specimen type	Average maximum load (N)	Average deflection at the centre of the sample(mm)	Average flexural stress (MPa)	Average flexural strain (mm/mm)	Average flexural modulus (GPa)
1	Sample with dichotomous vein structure	52.630	24.36	61.92	0.0449	1.38

2.3 Mesh Independency Checking

Boundary conditions:

The boundary condition used in the analysis is, deflection at a beam length $x = 0$ is 0, i.e. $y(0) = 0$, deflection at a beam length $x = l$ is 0, i.e. $y(l) = 0$, load is applied at the centre of the beam, deflection at centre is allowed in y-direction only. The element size of 0.22 mm was used as it is observed that after the element size of 0.25 mm the deformation is identical to the second digit after the decimal. A fine mesh consisting of 5,02,860 elements was used.

Validation is the process of checking the degree to which a simulated model is accurate to use in a real-world problem. In this study, the standard sample was simulated to determine the stiffness. The design was validated by performing a 3-point bending test on the fabricated part. Both the simulation and experimental results are compared and checked the error % in the simulated results as shown in Table 3 and Fig. 4.

Table 3 Validation of model

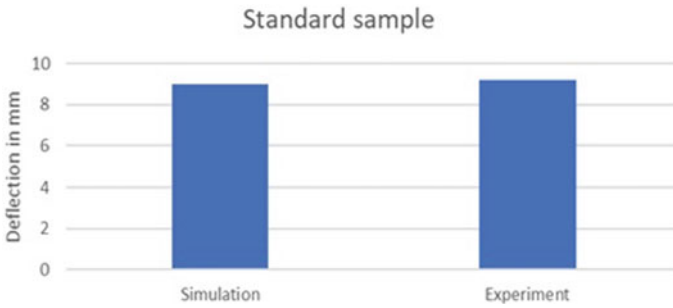| Sample	Deflection obtained from simulation up to 30N load in 'mm'	Deflection obtained from experiment up to 30 N load in 'mm'	% Error
Standard sample	8.9915	9.1910	2.17

Fig. 4 Comparison between experimental results and simulation results for three-point bending test up to 30 N load

It can be observed that the error obtained in the case of the standard sample is 2.17%. The reason for obtaining this error may be due to

- The human errors involved during the experiment and due to the limitations of the fabrication, technology employed, i.e. additive manufacturing in this work.
- Moreover, the difference is also occurred due to the material definition in ANSYS, where the value of Young's modulus is assumed as 2.4 GPa, but in reality, it can be in the range of 2 to 3 GPa.
- During analysis, the element size for the fine node was taken as 0.22 mm, which was obtained from the mesh independency checking of parts without any vein structures. The same element size was used for the other two samples also. However, the samples with leaf vein structures are more complex and hence the element size of 0.22 mm may not be the finer one to get an accurate result.
- From this, the FE model developed is evaluated and found to give satisfactory results with minimum error.

3   Results and Discussion

3.1   *Simulation of Aluminium 6061-T6 Parts*

The model developed earlier is used to simulate the effect of different leaf vein structures on the strength of the component made of aluminium 6061-T6 material. Table 4 represents the properties of aluminium 6061-T6 material. Three-point bending simulation was done on the rectangular bars consisting of the leaf vein structures. At the very first step, the material was defined, as it is not present in the material library of ANSYS Workbench. The material definition is done following the properties of aluminium 6061-T6 as given in Table 5. Four-leaf vein structures were evaluated, namely arcuate, dichotomous and parallel vein structure along with standard sample, i.e. without leaf vein structure as given in Table 5.

Table 4 Aluminium 6061—T6 material property

S. No	Properties	Magnitude
1	Young's modulus	6890 MPa
2	Tensile ultimate strength	310 MPa
3	Tensile yield strength	276 MPa
4	Density	2.7 g/cm^3
5	Poisson's ratio	0.33

Table 5 Specimen structures

S. No	Name of thestructure	Structure
1	Arcuate	
2	Dichotomous	
3	Parallel	

Simulation results are shown in Figs. 5, 6, 7 and 8 and tabulated in Table 6 for a load range of 0—30 N to compare and find out the most suitable vein structures among all. In the Table 6, simulation results of three-point bending test for a range of loading from 0 to 30 N are shown. The corresponding deformation values are directly collected from the solution module of ANSYS Workbench. From Table 6, it can be seen that the parallel and dichotomous leaf vein structures have shown the least value of deflection for the range of loading. The standard specimens, i.e. the specimen without any leaf vein structures have shown a deflection value of 2.7427 mm for a load of 30 N. On the other hand, samples with parallel and dichotomous leaf vein structures have shown deflection values of 2.1075 mm and 2.0383 mm, respectively, as shown in Table 7 and also in Fig. 10.

This is an indication of the stiffer design due to the application of the leaf vein structures upon the samples. The leaf vein structure acts as a support to withstand the external load and hence increases the resistance of the part to bending under the application of an external load. Load vs. deflection curve up to 30 N load of the above results has shown in Fig. 9. From the graph, it can be seen that the slope of load vs. deflection curve is highest or dichotomousand parallel leaf vein structures and is least for standard sample, i.e. the sample without any leaf vein structures. Higher the slope of load vs. deflection curve more is the stiffness. From the above results, two conclusions can be made.

The use of leaf vein structure has improved the stiffness of the parts as the leaf veins act as a support structure to withstand the external load and hence increase the resistance of the part to bending under the application of an external load.
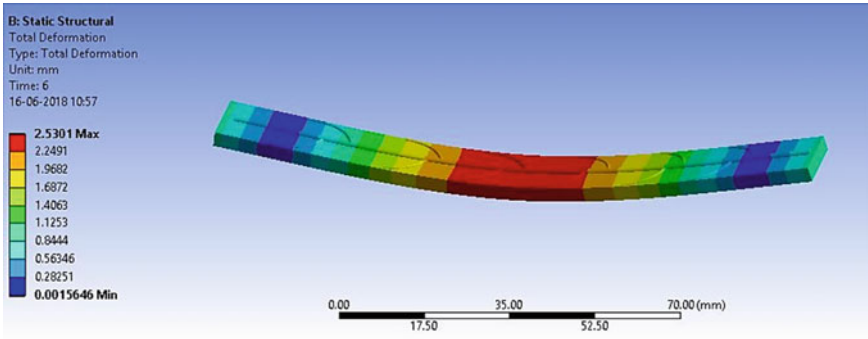
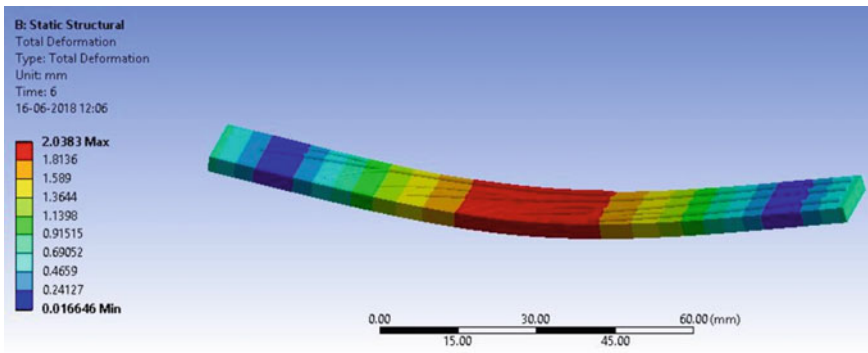**Fig. 5** Three-point bending simulation for Al 6061-T6 parts with arcuate vein structure

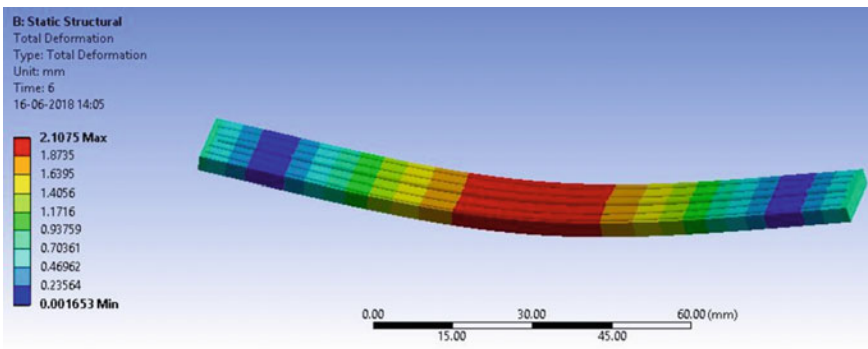**Fig. 6** Three-point bending simulation for Al 6061-T6 parts with dichotomous vein structure

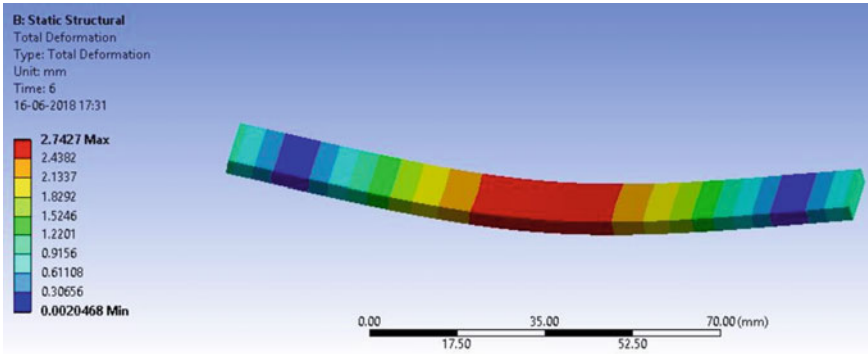**Fig.7** Three-point bending simulation for Al 6061-T6 parts with parallel vein structure

Fig. 8 Three-point bending simulation for Al 6061-T6 parts without any vein structure

Table 6 Summarized simulation results for Al 6061-T6 parts with different vein structures

S. No	Load	Arcuate	Dichotomous	Parallel	Standard
1	0	0	0	0	0
2	6	0.50602	0.40765	0.4215	0.54854
3	12	1.012	0.81531	0.843	1.0971
4	18	1.518	1.223	1.2645	1.6456
5	24	2.0241	1.6306	1.686	2.1942
6	30	2.5301	2.0383	2.1075	2.7427

Table 7 Summarized results for deflection

S. No	Samples with leaf vein structure	Aluminium 6061-T6 'mm'
1	Arcuate	2.5301
2	Dichotomous	2.0383
3	Parallel	2.1075
4	Samples without vein structure	2.7427

Among all the leaf vein structures, dichotomous and parallel structures are most suitable to improve the stiffness. The difference in the deflection value of the samples with the leaf vein structures under the application of the same amount of load is due to,

i. The distribution pattern of the leaf veins over the surface of the sample.
ii. Difference in the constituent veins present, i.e. in dichotomous structure, more than one primary veins are present which have more thickness than the secondary and tertiary veins; hence, it can provide more support to the applied load. Similarly, though in parallel vein structure, only one primary vein is present along
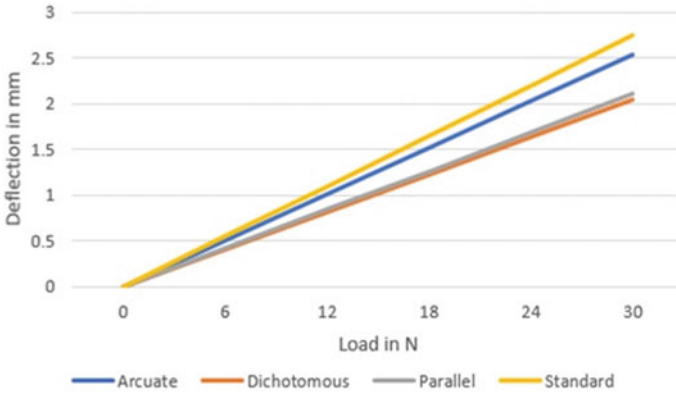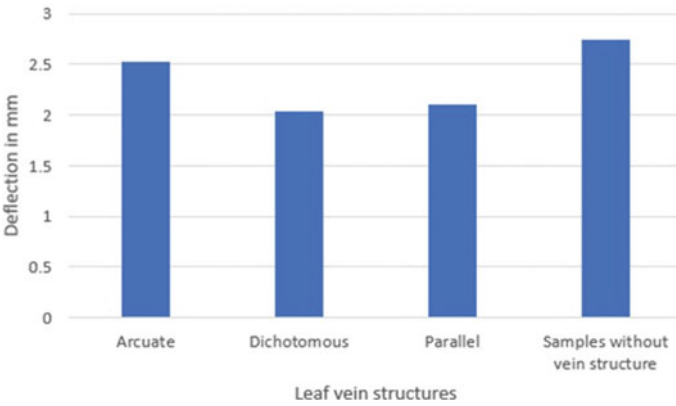
Fig. 9 Load versus deflection

Fig. 10 Deformation of aluminium 6061-T6 samples

with other secondary veins they are symmetrically distributed and in parallel with the primary veins. More than one primary veins are also present in rotated vein structure but their distribution is not uniform over the surface of the sample.

4 Conclusions

In this work, with the help of leaf vein structure, an approach was followed to improve the stiffness of the skin of aircraft wings. For this different leaf vein, structures were designed in CREO and studied in ANSYS Workbench to compare them and find the most suitable one among all. Standard samples were fabricated using additive manufacturing technology. Fabricated samples were subjected to three-point bending

test in a universal testing machine to compare the simulated results with the experimental one. After validation, leaf vein structures were simulated for aluminium 6061-T6 material. These designs are evaluated and the influence of leaf vein structure is studied.

- It is observed that the stiffness of the parts increased when vein structures were used. Almost all the types of vein structure can improve the stiffness as proved by the simulation results. Among all, the vein structures two most preferable vein structures are dichotomous veins and parallel veins.
- Simulation results are almost similar to the experimental results. It implies that the simulation model adapted is correct.
- Due to the change of material from PLA for the standard specimen to aluminium 6061-T6 for the samples, though the deflection value for all the samples under the same loading condition has decreased, which is due to the higher Young's modulus of aluminium 6061-T6 than PLA, the preference order for all the eight vein structures is same in both cases. It implies the material independency of the design.
- From the study, the dichotomous leaf vein structures are found to be more effective with less deformation.

References

1. Gibson, I., Rosen, D., Stucker, B.: In: Additive Manufacturing Technologies, 2nd edn. Springer, (2015). https://doi.org/10.1007/978-1-4939-2113-3
2. Anouar El, M. et al.: Mechanical properties of CF-reinforced PLA parts manufactured by fused deposition modeling. J. Thermoplastic Composite Mater. **34**(5), 581–595 (2021)
3. Algarni, M.: The influence of raster angle and moisture content on the mechanical properties of PLA parts produced by fused deposition modeling. Polymers **13**(2), 237 (2021)
4. Sehhat, M., Mahdianikhotbesara, H.A., Yadegari, F.: Impact of temperature and material variation on mechanical properties of parts fabricated with fused deposition modelling (FDM) additive manufacturing (2021)
5. Maurizio, G., Verna, E., Genta, G.: Effect of process parameters on parts quality and process efficiency of fused deposition modeling. Comput. Indus. Eng. **156**, 107238 (2021)
6. Keles, O., Blevins, C.W., Bowman, K.J.: Effect of build orientation on the mechanical reliability of 3D printed ABS. Rapid Prototyping J. **23**(2) (2017). Retrieved from https://doi.org/10.1108/RPJ-09-2015-0122
7. Lanzotti, A., Grasso, M., Staiano, G., Martorelli.: The impact of process parameters on mechanical properties of parts fabricated in PLA with an opensource 3-D printer. Rapid Prototyping J. **21**(5) (2015). Retrieved from https://doi.org/10.1108/RPJ-09-2014-0135
8. Mishra, S., Malik, B., Mahapatra, R.S.: Effect of external perimeter on flexural strength of FDM build part. Res. Article–Mech. Eng. (2017). https://doi.org/10.1007/s13369-017-2598-8
9. Liu, S., Shin, Y.C.: Additive manufacturing of Ti6Al4V alloy : a review. Mater. Des. **164**, 107552 (2019)
10. Tong, J., Bowen, C.R., Persson, J., Plummer, A.: Mechanical proper-ties of titanium-based Ti–6Al–4V alloys manufactured by powder bed additive manufacture. Mater. Sci. Technol. **33**(2), 138–148 (2017)

11. Herzog, D., Seyda, V., Wycisk, E., Emmelmann, C.: Additive manufacturing of metals. Acta. Mater. **117**, 371–392 (2016)
12. Hojati, F., Daneshi, A., Soltani, B., Azarhoushang, B., Biermann, D.: Study on machinability of additively manufactured and conventional titanium alloys in micro-milling process. Prec. Eng. (2019)
13. Frazier, W.E.: Metal additive manufacturing: a review. J. Mater. Eng. Perform. **23**(6), 1917–1928 (2014)
14. Ahmed, M., Islam, M., Vanhoose, J., Hewavitharana, L., Stanich, A., Hossain, M.: Comparisions of bending stiffness of 3D printed samples of different materials, November 11–17, (2016)
15. Li, B., Hong, J., Liu, Z.: Stiffness design of machine tool structures by a biologically inspired topology optimization method. Int. J. Machine Tools Manuf. 33–44 (2014). Retrieved from https://doi.org/10.1016/j.ijmachtools.2014.03.005
16. Sun, Z., Li, D., Zhang, W., Shi, S., Guo, X.: Topological optimization of biomimetic sandwich structures with hybrid core and CFRP face sheets. Compos. Sci. Technol. 79–90 (2017). Retrieved from https://doi.org/10.1016/j.compscitech.2017.01.029
17. Wang, J., Xie, H., Weng, Z., Senthil, T., Wu, L.: A novel approach to improve mechanical properties of parts fabricated by fused deposition modeling. Mater. Design 152–159 (2016). Retrieved from https://doi.org/10.1016/j.matdes.2016.05.078
18. ASTM D790—17.: Standard test methods for flexural properties of unreinforced and reinforced plastics and electrical insulating materials. (n.d.). Retrieved from ASTM International. https://www.astm.org/Standards/D790.htm